Measurement of the π-d elastic differential scattering cross section for momenta from 343 to 637 MeV/c

R. H. Cole, J. S. McCarthy, R. C. Minehart, and E. A. Wadlinger

Department of Physics, University of Virginia, Charlottesville, Virginia 22901

(Received 6 July 1977; revised manuscript received 24 October 1977)

The differential cross section for scattering of pions on deuterons was measured at LAMPF at laboratory momenta of 343, 441, 539, and 637 MeV/c, using an E-ΔE method to identify the recoil deuterons. Angles ranged from 40° to 160° in the center of mass system. The momentum resolution was $\sigma = \pm 3.5\%$ and the angular resolution was $\pm 1.70°$ in the laboratory system. The experimental method is discussed, and results are presented and compared with other experimental data as well as with various theoretical calculations.

NUCLEAR REACTIONS ^{2}H(π,π); $E = 230, 323, 417, 512$ MeV. D_2O, CD_2 targets. Measured $\sigma(\theta)$, $\theta = 40°$–$160°$, $\Delta\theta = 1.7°$, $\Delta p/p = 3.5\%$.

I. INTRODUCTION

With the successful operation of the new high intensity meson production facilities, it is now possible to study pion interactions with atomic nuclei at energies up to a few hundred MeV in much greater detail. The scattering of pions from deuterium is particularly attractive. Since the deuteron consists of only two nucleons, it seems probable that the π-d system will be amenable to very precise calculations based on the fundamental pion-nucleon parameters. Despite the simplifying features of the deuteron structure, its interaction with pions should exhibit effects that are important in pion interactions with more complicated nuclei. Included among such effects are multiple scattering, pion absorption, Fermi motion, off shell effects, and possibly the existence of isobars in nuclear wave functions. Details of the structure of the deuteron, particularly the D state and high momentum components of the wave function may also be important. Thus the pion-deuteron interaction is likely to provide a sensitive testing ground of our understanding of the behavior of a real pion in a nucleus.

In recent years a number of theoretical calculations have been published[1-6] representing a variety of techniques such as multiple scattering theory, the Glauber model, or the Faddeev three body equations. In principle, the multiple scattering theories are not strongly model dependent since details such as binding effects and complicated high order interactions seem to have only a small effect. However, in practice certain technical problems in carrying through the calculations have led different authors to different methods for treating the effects of Fermi motion, nucleon recoil, details of the deuteron structure, etc.

which in turn has led to significant differences in the final results.

The Faddeev equations allow an exact formulation of the three body problem in terms of coupled equations. Unfortunately, even at relatively low energies, a large number of coupled angular momentum states should be used, so that the magnitude of the computation increases rapidly as more states are coupled in, and so far, results using the Faddeev equations are not too satisfactory.

Despite the numerous calculational difficulties, theoretical work on the π-d system is being vigorously pursued by many people and a steady improvement in the quality of the results can be expected.

Experimental data are unfortunately still scarce and rather unsatisfactory due to difficulties arising from low cross sections and low beam intensities and to the weak binding of the deuteron, which has made it difficult to separate elastic and inelastic scattering.

At the Clinton P. Anderson Meson Physics Facility (LAMPF) we are engaged in a program to measure the differential cross section for π-d elastic scattering for energies ranging from 250 to 550 MeV. Other experiments at LAMPF are planned to measure the cross sections up to 300 MeV. In this paper we report the results of our first experiments. Only π^+ scattering was studied. Our measurements have an accuracy comparable to that of existing data[7-9] in the range of 180–330 MeV but extend to 515 MeV.

The experiment was performed in the early stages of LAMPF operation when the beam intensity was still relatively low ($\langle 7$ μA of proton current). Consequently, we had to employ a rather large momentum spread in the pion beam and

were forced to operate with a rather large beam
spot on the target. Instabilities in the beam di-
rection and composition also contributed to in-
accuracies in the result. The main limitation in
accuracy, however, in most of the data is due
to the low counting rate.

II. EXPERIMENTAL METHOD

Besides detecting the scattered pion, we iden-
tified the recoil deuteron to guarantee the elastic
nature of the scattering. The experimental ar-
rangement is shown in Fig. 1. The high intensity,
high energy pion beam (designated P^3 at LAMPF)
with a momentum spread $\Delta p/p = 8\%$ full width at
half maximum was focused onto thin targets of
CD_2 or D_2O (~2.5–12.5 mm) for π-d scattering
measurements and on CH_2 or H_2O targets of sim-
ilar thicknesses for π-p normalization measure-
ments. A magnetic spectrometer served to mea-
sure the scattering angle and the pion momentum.
The recoil particle was detected in a second
spectrometer designed to measure the recoil angle
and to identify it by the E-ΔE method. Our data

at each setting of the spectrometer were combined
to result in an angular bin with a width given by
$\Delta\theta = 1.7°$.

In both spectrometer arms the particle trajec-
tories were measured by a set of helical multi-
wire proportional counters, as described by Lee
et al.[10] Six assemblies, each consisting of a
separate x and y detector, were used. Each de-
tector was made of an anode plane consisting of
parallel gold coated tungsten wires (20.3 μm diam)
separated by 4 mm, around which a helix with a
2 mm pitch was wound to form two parallel cathode
planes separated from the anode by 4.8 mm. The
charge collected on the anode plane after the pas-
sage of an ionizing particle induces a pulse on the
helix plane, which then travels toward each end
of the helical delay line. The propagation time
to each end serves to define the position of the
ionizing event with a resolution of approximately
1 mm.

Two helical chamber assemblies were used at
the entrance side and two more were used at the
exit side of a bending magnet with a gap 76.2
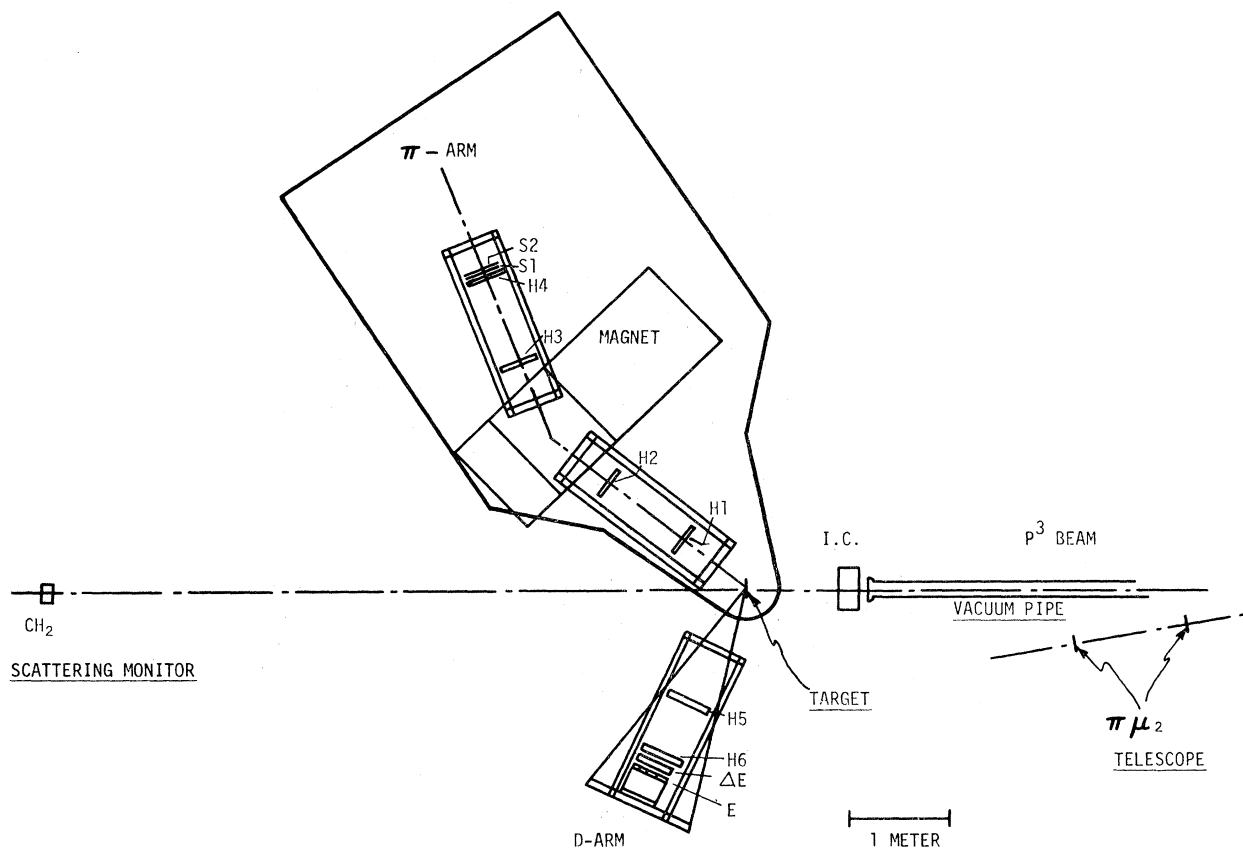cm wide by 101.6 cm long and 15.2 cm high. Any

FIG. 1. Diagram of experimental arrangement.

three of the four horizontal, or x, coordinates determined by the chambers are sufficient to determine the momentum to first order. The spectrometer was designed for a nominal bending angle of $30°$.

The two entrance chambers ($H1, H2$) on the pion spectrometer served to determine the pion scattering angle and the two chambers ($H5, H6$) on the deuteron spectrometer measured the recoil angle. Actually, any three of these four chambers are sufficient to determine both the scattering and recoil angle if one assumes that the two particles originate from a common point in the target.

The pion detectors were mounted rigidly to the bending magnet which in turn was supported by a large motor driven spectrometer cart, free to rotate around a pivot located at the target position. The deuteron detectors were mounted on a much lighter cart constructed of aluminum I beams and pivoted by hand around the same point as the pion arm.

The CD_2 target was 10 cm $\times$ 10 cm $\times$ 0.254 cm, the CH_2 targets were either 15 cm $\times$ 15 cm $\times$ 0.20 cm or 10 cm $\times$ 10 cm $\times$ 0.32 cm, with the second one most commonly used. The water targets were made by adding 2% agar-agar to distilled water and allowing the mixture to jell between two sheets of cellophane supported by an aluminun frame. Two targets were used, both being 15 cm by 20 cm wide, with thicknesses of 0.635 cm and 1.27 cm. The need for a variety of targets arose from the fact that thin targets were needed at small pion scattering angles when low energy recoil deuterons were produced and thick targets were required at larger pion scattering angles where the cross section is much lower. The targets were mounted at various angles to the beam to minimize the effects of energy loss and multiple scattering for the emerging pion and deuteron.

The relative pion beam intensity was monitored by three separate systems. The primary monitor was a cylindrical parallel plate ionization chamber, 20 cm in diameter, filled with argon gas at atmospheric pressure. The current from the chamber was collected by a current digitizer (ORTEC model 439) whose digital output was fed to a CAMAC scaler for computer (PDP 11/20) readout.

A second monitor consisted of a three element scintillation counter telescope designed to detect particles scattered at $75°$ in a vertical plane from a CH_2 target located approximately 3 m downstream from the primary scattering target. Because of the large scattering angle, this system was relatively insensitive to muons in the beam, but it was sensitive to changes in the beam di-

rection

The third monitor[11] was made of two circular scintillators (1.27 cm in diameter) separated by 50 cm and placed upstream of the target to measure particles emerging at angles from $2.8°$ to $5.7°$ with respect to the beam. This system was designed to detect muons from pion decay, but it was also sensitive to low energy protons and pions scattered from pole pieces and the vacuum pipe.

Except for isolated cases, the three monitors showed long term consistency of $\pm 2\%$ to $\pm 5\%$. In most of the inconsistent cases, the difficutly could be attributed to known changes in the beam conditions, or to a malfunction of one of the three monitors. In determining the beam normalization, our usual procedure was to average the valid monitors. The average value tended to agree with the ion chamber itself to $\pm 2\%$ except for a run at 441 MeV/c where the agreement was $\pm 4\%$ and for a run at 537 MeV/c for which the agreement was $\pm 5\%$. The absolute calibration was obtained from π-p scattering runs, a procedure to be described later.

The momenta measured in our spectrometer were consistently lower than expected. Later studies of the beam by Werbeck and Macek[12] showed that the central momentum was 2% lower than predicted. The momenta given here contain that correction. We estimate that the uncertainty in the beam momentum is less than 1%, which contributes a systematic error of less than 3% in our cross sections.

The size of the beam at the target is important in the evaluation of the solid angle. Because the target was located 10 m from the last quadrupole magnet in the P^3 beam, it was not possible to obtain beam spots smaller than 10–12 cm wide by 8–9 cm high, full width at the base. When a beam was first set up, two helical chambers were placed in the beam to observe the distribution. Because of the high beam rates and because of the large component of decay muons as well as protons, this method was of somewhat limited value in determining the beam size. However, it was usually consistent to within ± 1 cm with the method used in the analysis, namely, extrapolation of trajectories back to the target.

To identify the recoil particle, an E-ΔE system was placed at the end of the deuteron spectrometer. Two different ΔE systems were employed interchangeably, one thin and the other thick. The thin detector, used for identifying low energy recoil particles, consisted of five planar multiwire porportional counters in series. Each one was made of an anode plane at high voltage with a ground plane on each side. The anode plane

was formed of 20.3 μm gold-plated tungsten wires separated by 8 mm. The ground planes were made of 25.4 μm stainless steel wires separated by 1 mm and oriented perpendicular to the direction of the anode wires. The separation between the anode and each cathode plane was 1.27 cm. The five proportional counters were placed in a box, which was continously flushed at atmospheric pressure (0.76 bars at Los Alamos) with a mixture of 10% CO_2 in argon. The signals from the anode planes were amplified by FET preamplifiers followed by linear amplifiers whose output pulse heights were digitized by gated 1024 channel analog-to-digital converters (ADC's) connected to the PDP-11/20 computer.

The second ΔE system was a set of scintillation detectors, each scintillator being 5.08 cm wide by 25 cm high and 2.0 cm thick. Three such detectors were used in coincidence with the NaI energy detector. The signals from the detectors were coupled directly into the ADC circuits connected to computer readout.

To measure the energy of the recoil particles, we used a NaI detector, 1.27 cm thick and 12.5

cm in diameter, which stopped deuterons up to an energy of 75 MeV. More energetic deuterons were moderated with Al or Fe plates of appropriate thickness before entering the $E/\Delta E$ system. The thickness of the NaI was chosen as a compromise between two factors. For optimum detection of deuterons over a large range of energies, the ideal thickness would have been more like 4–6 cm. However, the background from neutral radiation and low energy particles is proportional to the thickness so that it was believed that the chosen size would be better. With the thickness chosen, we had only minor trouble with pile-up of the pulses. The signals from the NaI were sent directly into a gated ADC monitored by the computer.

Electronic Logic

The electronic logic used to define an event is shown in Fig. 2. For each helical chamber, the x and y anode signals were combined in an "OR" circuit. One output of the "OR" circuit was used in the event logic. The other output was delayed and then strobed with an event trigger to start
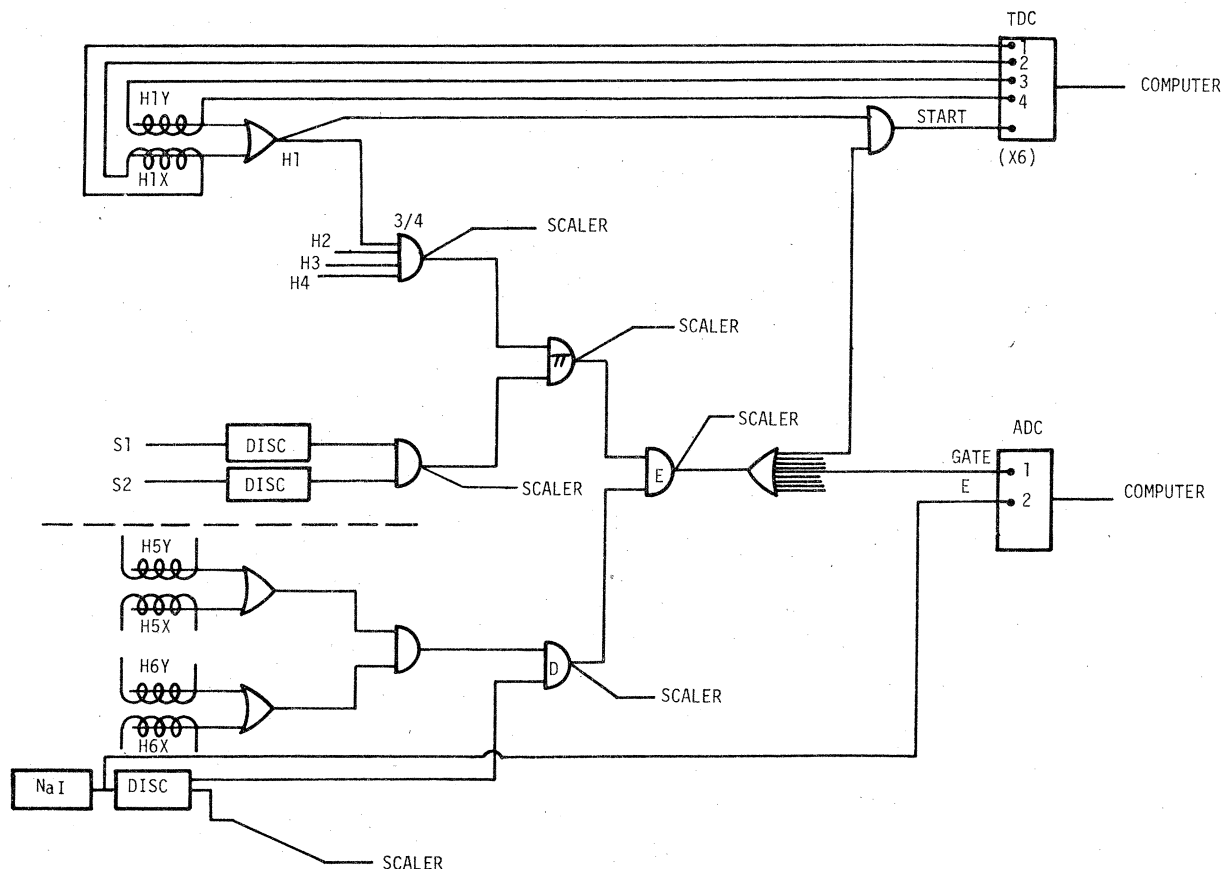

FIG. 2. Diagram of electronic logic arrangement.

a time digitizer circuit (TDC), used to measure
the propagation times for the x and y helix signals.
On the pion arm, the four helical chamber logic
signals were combined in a coincidence circuit
set to respond when any three were in coincidence.
The output of this circuit was put into coincidence
with the coincidence signal from a telescope of
two scintillation counters, ($S1$, $S2$) located just
beyond $H4$. These two scintillators were each 30
cm high and 47 cm wide. The resulting signal
defined a "pion." On the deuteron spectrometer
the x and y planes in each chamber were com-
bined in separate "OR" circuits whose outputs
were added in a coincidence circuit. This coin-
cidence signal was added in coincidence to the
NaI signal to define a "deuteron" signal which was
then combined in coincidence with the "pion" signal
to obtain an "event" signal. The event signal provid-
ed gates for reading out the helical chamber po-
sition information and the E-ΔE pulse height val-
ues. When the scintillator ΔE system was used,
a latch circuit was used to specify which of the
ΔE counters was in coincidence with the event.

Two six-fold CAMAC scalers recorded various
counting rates in the logic chain as well as the
rates from the three monitors.

Data Analysis

The data were sorted according to various cri-
teria that should be met by an elastic π-d scat-

tering. The events were first tested to determine
whether the E-ΔE information was consistent with
a recoil deuteron. The $\ln(\Delta E)$ and $\ln(E)$ were
plotted, such as shown in Fig. 3(a). The deuteron
region in this figure is circled. By comparing
to the background run taken with a CH_2 target,
shown in Fig. 3(b), it is apparent that the deuteron
recoils are easily separated in this run. Not all
runs were so clean-cut because the signal to noise
ratio became rather small at large angles.

Events satisfying the E-ΔE cut were analyzed
by using the helical chamber timing information
to calculate for each chamber the spatial coordin-
ates, which were then used to reconstruct the tra-
jectories. To test the validity of the two timing
signals for each helical plane, we first added
them to form a sum that should be equal to the
transit time across the entire helical delay line.
If the summed time was inconsistent with the prop-
agation time of the chamber delay line, we tagged
the corresponding coordinate as being faulty. The
two propagation times were used to calculate a
position with the formula

$$x = v(t_1 - t_2) + x_0 ,$$

where v is half the propagation velocity and x_0
is a correction for misalignment of the center of
the chamber. Both v and x_0 were determined by
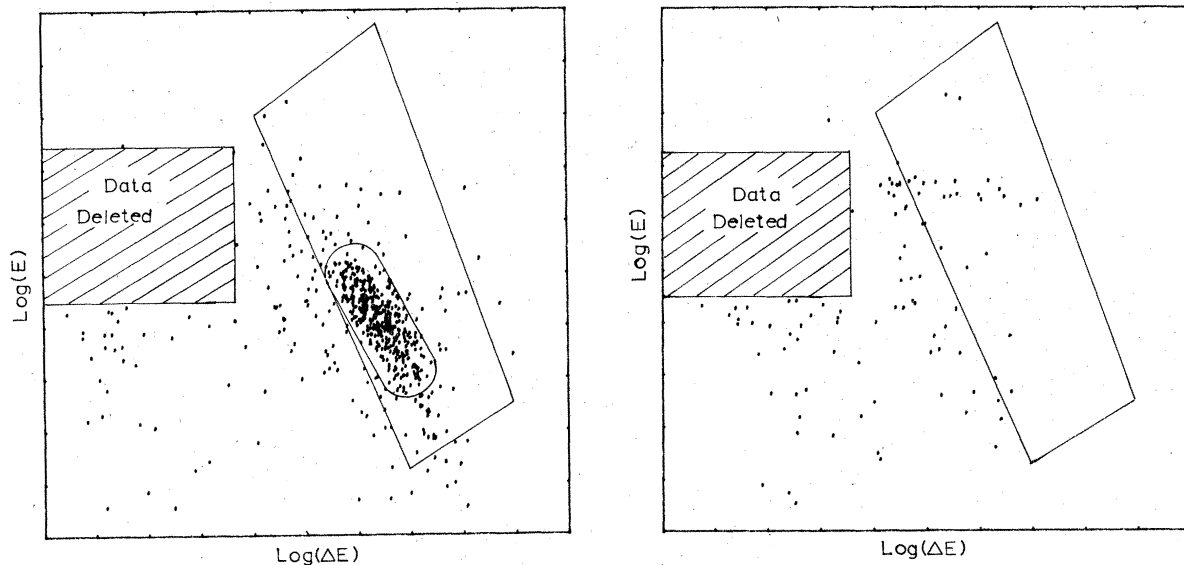a separate calibration procedure using an ^{55}Fe
line source.

FIG. 3. (a) Scatter plot of log(E) vs log(ΔE) for a run with incident pions with momentum P_{lab} = 343 MeV/c on a CD_2
target. The deuterons recoiling from π-d elastic scattering are associated with the points enclosed in the elliptical
region. The data selected for further analysis are enclosed in the quadrilateral figure. A large number of proton re-
coils were eliminated in a preselection process by deleting the data from the region marked "data deleted." (b) Same
as (a) except the data were obtained with a CH_2 target. These data are the background for (a). To normalize to 3(a)
multiply 3(b) by 1.90.

An error was assigned to the above calculated value of x, according to:

$$\sigma_x = v[(t_1 + t_2) - t_s]/\sqrt{12} ,$$

where t_s = expected summed time.

The formula was arbitrarily chosen so that for complete failure of the plane ($t_1 = t_2 = 0$) we obtain $\sigma_x = w/\sqrt{12}$, where w is the half width of the plane, which is consistent with the standard deviation expected for a square distribution of width w. We used half-width since only about half the sensitive area was actually filled by the particles. In addition, when the above formula yielded σ_x <1 mm, we set $\sigma_x = 1$ mm, which is consistent with other measurements for the resolution of our chambers.

Besides the helical chamber data for particle coordinates we also know that both particles originated in the target and that the recoil particle entered the NaI detector. Although the target and NaI coordinates are known with very poor resolution, we included them in the analysis, assigning to them an error $\sigma = w/\sqrt{12}$, where w was the full width of the target or NaI detector.

We fit the coordinates and their errors to straight lines emerging from a common vertex in the target by using a least squares minimization program. One line defined the scattered pion and the other defined the recoil nucleus. These trajectories served to define the scattering and recoil angles. The momentum of the scattered pion was determined from the fitted pion trajectory into the magnet and from the coordinates in the two chambers on the exit side of the magnet. The orbit through the magnet was calculated by assuming a uniform field with effective length determined from field maps.

The scattered pion momentum and the scattering and recoil angles were combined to calculate the momenta of the recoil particle and the incident pion, assuming elastic scattering. From these measured and derived quantities we calculated the mass of an assumed third body in the final state (missing mass), which should vanish for elastic scattering.

The analyzed data were divided into two classes according to a procedure designed to sort out events which had enough good measured coordinates to make accurate determinations of all trajectories. For each plane, the summed time was compared with the expected value. We observed a strong peaking around the expected value for chambers working well with low beam rates. If the summed time fell inside this peak, the coordinate for the helical plane was considered good; otherwise the coordinate was tagged as being of low reliability. A poor summed time could be caused by more than one ionizing event during the sensitive time of the chamber, or by a weak signal. For an event to be acceptable, we required at least three good x coordinates in the chambers $H1$, $H2$, $H5$, and $H6$ which define the scattered and recoil trajectories. In addition, we required at least two good x values on one side and at least one on the other side of the magnet for good determination of the momentum. If the momentum could not be considered well-determined in this way, the event was not accepted. Distributions were made of the unacceptable events as well as the good ones. They were generally consistent but the accepted events yielded higher resolution and smoother distributions. We, therefore, used only the acceptable events in determining the fraction of events that represented elastic scattering. Typically, the fraction of unacceptable events ranged from 15% to 50%, depending on operating conditions of the chambers and on background rates, which were angle dependent.

To reduce the distributions to the number of elastic scatterings in a run, we used the average of two procedures. The distribution of the square of the missing mass, M^2, was cut off at a value well away from the peak at $M^2 = 0$. Empirically, it was found that a cutoff at $M^2 = 300$ $(MeV)^2$ would result in less than 1% of the deuteron events being discarded. The same cut was made on background
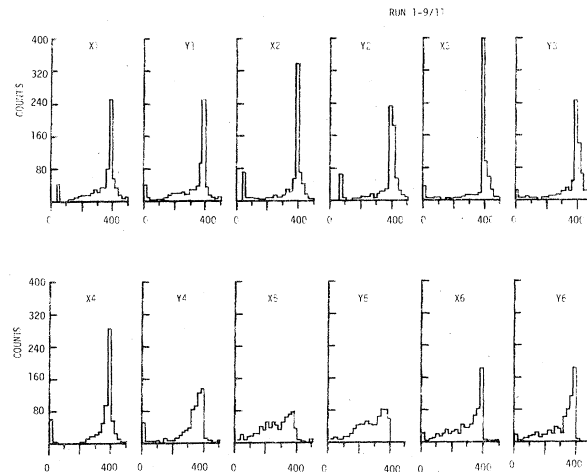

FIG. 4. Histograms of the sum of the two propagation times for each helical chamber plane. The sharp peaks mark the value of the summed time corresponding to the propagation time across the chamber. Data to the left of the peak can arise from more than one particle passing through the chamber. Data to the right of the peak are due to variations in the start signal for the time digitizer that result from the logic used in the experiment. An arbitrary number has been added to the summed time for each plane to shift the peak into channel 400.

data and then the background was subtracted from the deuteron run to obtain the π-d elastic events. The same type of rough cut and subtraction was done for the momentum distribution. The two procedures were usually consistent. In a few cases, where inconsistency resulted, we decided to keep the momentum results. In these cases, the momentum distribution looked normal, whereas the missing mass distribution showed poor resolution. The determination of momentum requires only three out of four coordinates on the pion spectrometer, whereas the missing mass calculation depends on the deuteron trajectory as well.

The analysis can be illustrated by a detailed examination of the data taken for a particular angle and momentum, which is done in Figs. 4-9.

The momentum of the incident pion beam was 441 MeV/c. Run No. 1 was made with a 0.64 cm thick D_2O target and with the pion spectrometer
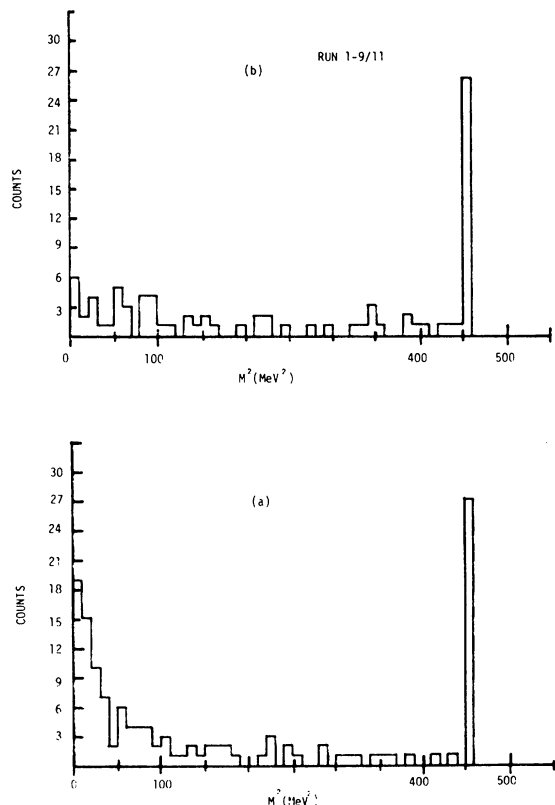
FIG. 5. Plots of the square of the missing mass for events surviving the E-ΔE deuteron cut. (a) Data with a sufficient number of helical planes with acceptable summed times to make a reliable kinematical analysis. (b) Data with an insufficient number of helical planes with acceptable summed times to make a reliable kinematical analysis.
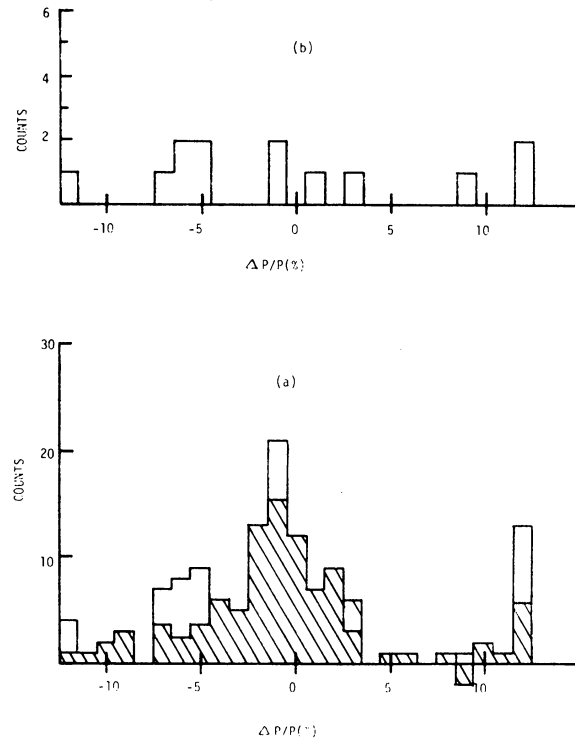

FIG. 6. (a) Momentum distribution of elastic π-d events. The shaded areas show the distribution obtained after normalizing the background of Fig. 6(b) and subtracting it. (b) Background distribution for Fig. 6(a), obtained with an H_2O target. The data should be multiplied by 2.77 to normalize them to Fig. 6(a).

set at 80°. Run No. 2 was obtained with D_2O target replaced by a 0.64 cm H_2O target, with all angles set the same as for run No. 1. In run No. 3, the pion angle was changed to 70° in order to detect the π-p events from the H_2O targets. In all three runs, the deuteron arm was set at 43°.

In Fig. 4 we display histograms of summed times for run No. 1, made at the beginning of a cycle. Planes 9 and 10 were working rather poorly in this run, as can be seen from the width of the summed time distribution.

A typical plot of the missing mass function for events surviving the E-ΔE cut is shown in Fig. 5. Those events for which a sufficient number of chambers worked to give reliable trajectories through the entire system display a peak at 0 which serves as corroboration of the validity of the E-ΔE cut. A plot of M^2 for the background run exhibits no evidence of such a peak, and neither do other cuts in the E-ΔE plot.

The same events are also distributed according to the momentum of the scattered pion, with histograms shown in Fig. 6. The events from run No. 1 are peaked around the expected value, while
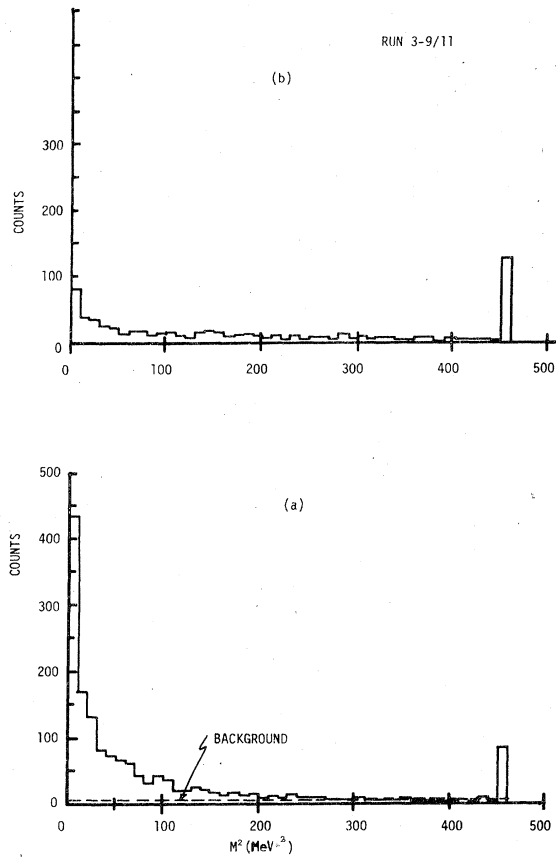
FIG. 7. Square of the missing mass for π-p elastic
scattering data, obtained with an H_2O target. (a) Data
with sufficient number of helical planes with acceptable
summed times to make a reliable kinematical analysis.
The dashed curve shows the assumed background. (b)
Data with an insufficient number of helical planes with
acceptable summed times to make a reliable kinematical
analysis.

the background run shows little evidence for any
peaking. The background can result from $(\pi, \pi d)$
reactions in ^{16}O and from $(\pi, \pi p)$ events in both
deuterium and ^{16}O if some of the protons are in-
correctly identified as deuterons. For these par-
ticular data the missing mass spectrum could have
been cut off at a point less than 300 $(MeV)^2$, but in
some runs 5–10% of the data lay between 150 and
300 $(MeV)^2$. To reduce possible bias, the cut was
made at 300 on all runs.

The data were normalized to the incident pion
flux by comparison to π-p elastic scattering data
obtained with H_2O or CH_2 targets. In general, we
did not take background runs for the π-p data be-
cause the background was small and could be es-
timated with sufficient precision by fitting a
straight line to the tails of the distributions. As
an example, we show the missing mass spectrum

and the momentum distribution along with the es-
timated background in Figs. 7 and 8.

In order to calculate the solid angle of the ap-
paratus, it is necessary to know the beam dis-
tribution. The target coordinates were obtained
from the pion and deuteron trajectories. The
widths and heights of the shapes expected from
the first-order magnet transport theory were
adjusted to fit the data. The solid angle was cal-
culated with a Monte Carlo program which also
included effects of multiple scattering and energy
loss. The angular distribution in the beam was
not measured; instead we used a distribution con-
sistent with transport[13] calculations for the P^3
beam. The solid angles were calculated to a sta-
tistical accuracy of approximately 5%. The quality
of the data did not justify more accurate calcula-
tions. Changes in the assumed beam size com-
parable to the uncertainties of our measurement
resulted in changes of at most 3–5% (generally
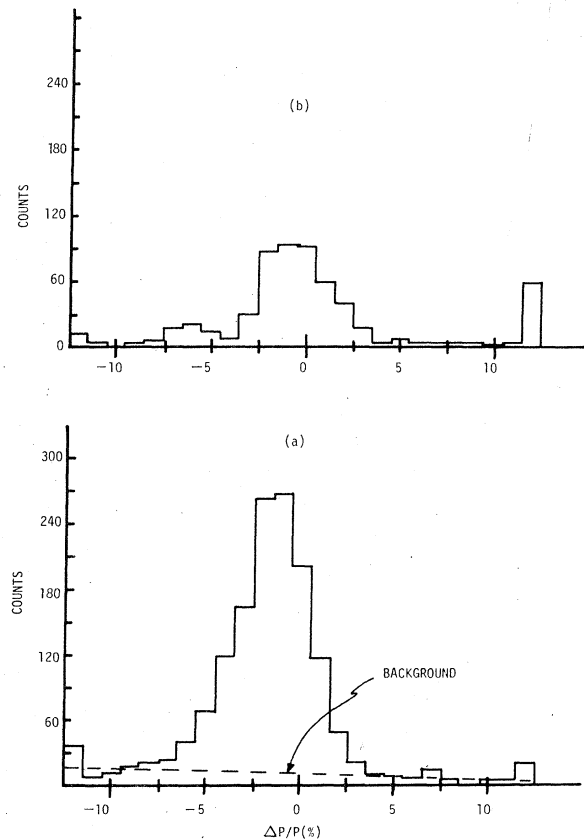less) in the final π-d cross sections and thus made

FIG. 8. Histogram of the momenta of the scattered
pions for the π-p elastic scattering events shown in
Fig. 7. The dashed curve in Fig. 8(a) shows the assumed
background obtained from the tails of the distribution.
The significance of (a) and (b) is the same as for Fig. 7.

negligible contribution to the total uncertainty in the cross sections.

A correction for pion decay in the pion spectrometer was calculated by determining the probability for decay of the pion anywhere before the proportional chamber, $H3$, and assuming that for such a case the event would be lost. This is consistent with results of a Monte Carlo calculation. Since the magnitude of the correction is comparable for the π-p and π-d data, an error in the correction has a small effect on the π-d cross sections, which are obtained as ratios of π-d to π-p results. The ratio of the π decay correction for deuteron and proton scattering ranges between 0.96 and 1.04 for our data, except at 156° in the laboratory where the ratio was 0.93 for 343 MeV/c and 441 MeV/c.

Inelastic reactions by the deuterons in the spectrometer result in their being undetected or detected with pulse heights in the E-ΔE system outside the region for deuterons. The break-up probability is roughly proportional to range. It has been measured at 27 MeV by Eisberg et $al.$[14] and at higher energies by Millburn et $al.$[15] At 27 MeV the loss is only about 1%, which is negligible for our data, but at our highest energies the loss reaches 30%. The measurements of Millburn have been used to correct our data for this loss.

The π-p normalization data were also corrected for proton inelastic reactions in the spectrometer. In most cases the correction was of the order of a few percent, with the largest correction being 11% for a point measured at 637 MeV/c. The inelastic cross sections were obtained from a compilation of McGill et $al.$[16] for energies below 60 MeV and from compilations of Pollack and Schrank[17] and Measday and Richard-Serre[18] at higher energies.

The errors in our cross sections due to errors in the deuteron break-up measurements of Millburn et $al.$[15] are always less than 2%. The error due to correction for scattering of the recoil proton is always less than 2% and reaches that only for the 637 MeV/c data for which other errors are much larger.

No correction was made for pion nuclear scattering in the pion spectrometer because the amount of material (0.64 g/cm² equivalent of Al) encountered by the pion is so small that even using the maximum π-nucleus total cross section observed in the 3-3 resonance region,[19] only 2% of the pions interact. When the ratio of πd/πp is taken, the correction would be reduced below the 1% level.

To obtain the absolute calibration of the beam monitors we used the π-p cross sections obtained from the energy dependent phase shifts of Roper, Wright and Feld,[20] which extended up to energies of 700 MeV. These calculated cross sections are consistent with most experimental data, including the very accurate data of Bugg et $al.$[21] However, they tend to produce cross sections as much as 10% higher than observed by Gordeev et $al.$[22] for momenta from 400 to 590 MeV/c. In general, their results are lower than other existing data and phase shift fits. Until this discrepancy is confirmed by others, it seems premature to use their results in normalizing our data.

The absolute calibration of the beam monitors using the π-p data varied as much as ±15% from angle to angle in a sequence of runs at a given energy. This variation is partly due to uncertainties in the calculation of the effective solid angle (about 5%), and to uncertainties in the nuclear scattering corrections (<5%). We can also expect
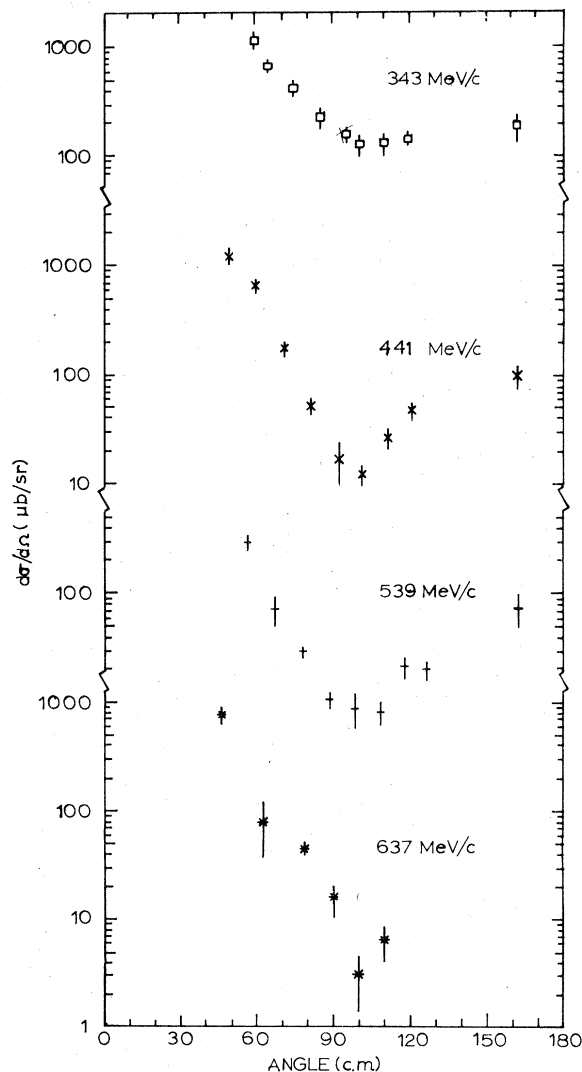

FIG. 9. Measured differential cross sections in the c.m. system.

problems from variations in beam geometry and compostion which will have different effects on the, response of the three monitors. These effects tend to cancel out when the ratio of $\pi d/\pi p$ is taken. However, we estimate that there remains at each point a random systematic error of 10%. This error has been combined with the statistical error in the final results.

III. RESULTS

The results are shown in Fig. 9 where we have plotted the cross sections for each momentum. For the most part, the data were consistent from one run to another. At 343 MeV/c there was some indication of a systematic difference between two separate runs with two of five angles showing a shift of $2\frac{1}{2}$ standard deviations. We have been unable, however, to explain the discrepancies and have chosen to treat them
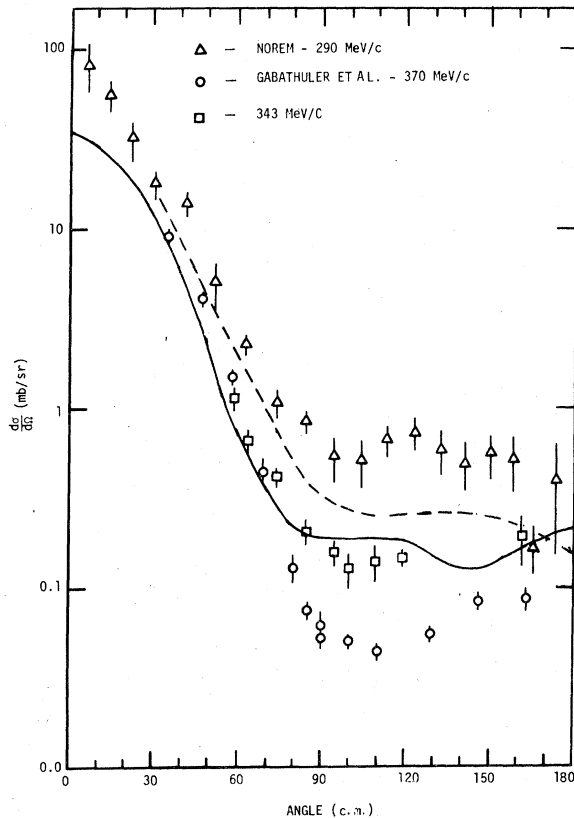
FIG. 10. Differential cross sections in the c.m. system obtained by Norem (Ref. 7) at $P_{lab} = 290$ MeV/c and by Gabathuler et al. (Ref. 8) at $P_{lab} = 370$ MeV/c along with our data at $P_{lab} = 343$ MeV/c. The dashed line is the calculation of Ferreira et al. (Ref. 1). The solid line is the calculation of Rinat and Thomas (Ref. 5) at 370 MeV/c.
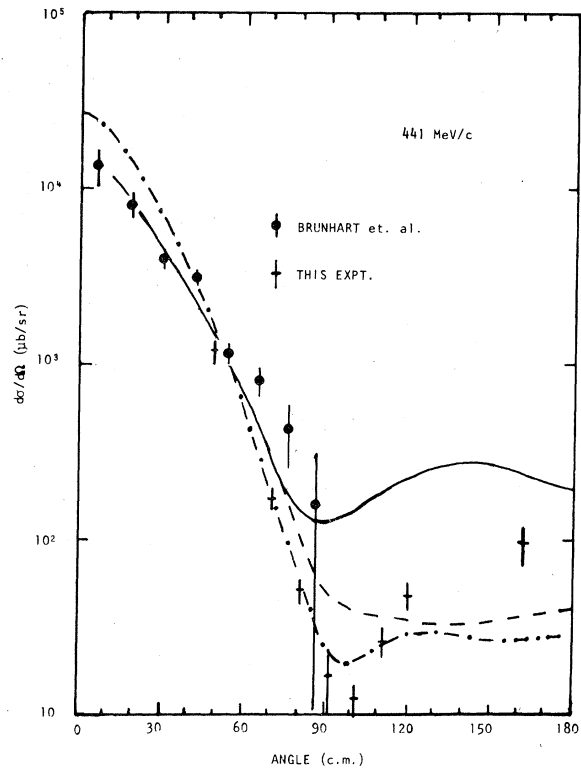

FIG. 11. Differential cross sections in the c.m. system showing both our data on π^+-d scattering at 441 MeV/c and the data of Brunhart et al. (Ref. 9) for π^--d scattering at 448 MeV/c. The solid line is the calculation of Schiff and Tranh Thanh Van (Ref. 4). The dashed line is the calculation of Ferreira et al. (Ref. 1). The dotted line is the calculation of Hoenig and Rinat (Ref. 3) at $P_{lab} = 438$ MeV/c.

as statistical fluctuations and averaged the results of the different runs, increasing the errors to include the range of the measurements. The averaged cross sections are listed in Table I. In Fig. 10, we show our data at 343 MeV/c along with the results of Norem[7] at 290 MeV/c and Gabathuler et al.[8] at 370 MeV/c. In comparison to Gabathuler et al.,[8] our data at 343 MeV/c tend to be low at the forward angles. It should be noted that at the forward angles at this energy, the correction for deuteron absorption tends to be large because the deuterons have low energy. However, the amount of material in the deuteron spectrometer is well known and we cannot account for the discrepancy with Gabathuler et al. through this mechanism. In our next experiments we plan to use a gas target and very thin detectors to observe the recoil deuteron at these angles to help resolve this question.

At 448 MeV/c, Brunhart et al.[9] measured cross

TABLE I. π-d elastic scattering cross sections.

| $P_{lab}=343$ MeV/c					$P_{lab}=441$ MeV/c				
Lab. system		c.m. system			Lab. system		c.m. system		
Angle	$d\sigma/d\Omega$ (mb/sr)	Angle	$d\sigma/d\Omega$ (mb/sr)		Angle	$d\sigma/d\Omega$ (mb/sr)	Angle	$d\sigma/d\Omega$ (mb/sr)	
50.6	1.41 ±0.24	58.5	1.16 ±0.20		40.7	1.61 ±0.27	48.9	1.21 ±0.20	
55.4	0.80 ±0.11	63.8	0.67 ±0.09		49.7	0.843 ±0.12	59.2	0.66 ±0.09	
64.9	0.48 ±0.08	74.0	0.42 ±0.07		59.8	0.206 ±0.029	70.4	0.173 ±0.024	
74.8	0.24 ±0.05	84.4	0.23 ±0.05		69.7	0.058 ±0.010	81.0	0.052 ±0.009	
84.9	0.160 ±0.024	94.7	0.160 ±0.024		80.0	0.0176 ±0.0072	91.7	0.0170 ±0.0070	
89.9	0.126 ±0.024	99.7	0.129 ±0.028		89.2	0.0120 ±0.0025	100.9	0.0124 ±0.0026	
99.7	0.122 ±0.025	109.2	0.133 ±0.030		99.6	0.0239 ±0.0048	110.9	0.0266 ±0.0053	
109.8	0.127 ±0.010	118.8	0.146 ±0.018		109.7	0.0404 ±0.0071	120.4	0.0480 ±0.0084	
158.3	0.141 ±0.041	161.7	0.195 ±0.057		158.1	0.065 ±0.015	162.1	0.097 ±0.023	
$P_{lab}=539$ MeV/c					$P_{lab}=637$ MeV/c				
46.0	0.392 ±0.064	56.5	0.291 ±0.048		36.2	1.16 ±0.21	46.2	0.78 ±0.14	
55.3	0.095 ±0.028	67.1	0.075 ±0.022		50.0	0.107 ±0.055	62.7	0.080 ±0.040	
65.0	0.035 ±0.006	77.8	0.030 ±0.004		64.4	0.052 ±0.009	78.9	0.045 ±0.008	
74.7	0.0119 ±0.0024	88.1	0.0110 ±0.0020		74.7	0.016 ±0.005	89.9	0.015 ±0.004	
84.7	0.0090 ±0.0032	98.3	0.0091 ±0.0032		84.7	0.0029 ±0.0016	100.0	0.0030 ±0.0016	
94.9	0.0075 ±0.0019	108.2	0.0082 ±0.0021		94.9	0.0057 ±0.0021	109.9	0.0064 ±0.0024	
105.1	0.0176 ±0.0034	117.8	0.0209 ±0.0041						
114.7	0.0158 ±0.0029	126.4	0.0201 ±0.0036						
157.7	0.046 ±0.015	162.4	0.073 ±0.025						
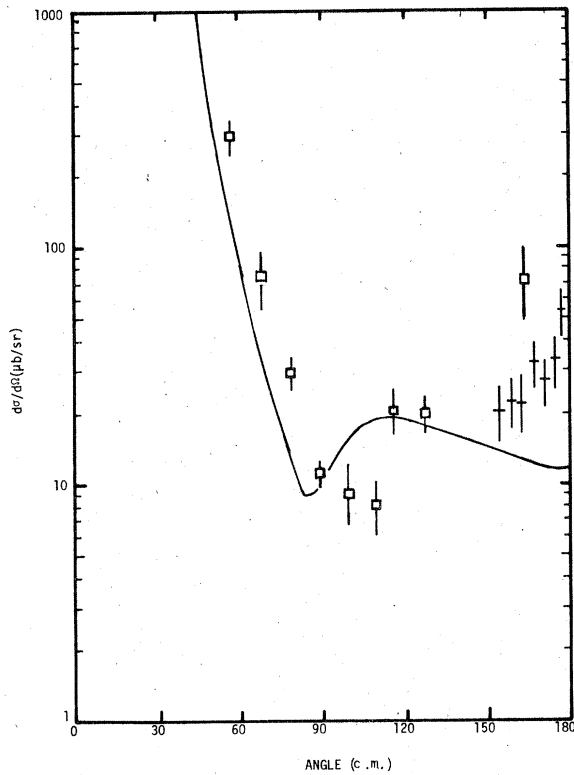
FIG. 12. Differential cross section in the c.m. system at $P_{lab}=539$ MeV/c. Our data are shown with open squares and the data of Schroeder *et al.* (Ref. 23) are shown with crosses. The solid line is the calculation of Hoenig and Rinat (Ref. 3) for $P_{lab}=573$ MeV/c.

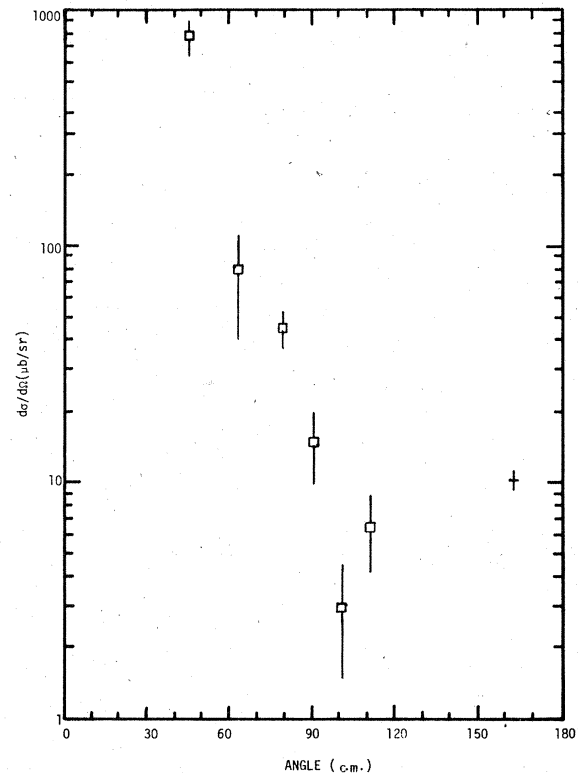FIG. 13. Differential cross section in the c.m. system for $P_{lab}=637$ MeV/c. Our data are shown in open squares. The cross point was obtained by interpolation from the data of Schroeder *et al.* (Ref. 23).

sections for π^--d elastic scattering in a bubble chamber. Beyond $\theta = 70°$, the number of events observed by them became too small to set more than an upper limit. Their data at smaller angles are shown combined with ours in Fig. 11. Our measurements are lower than theirs and there is a tendency for our measurements to decrease more rapidly than theirs as the angle increases.

Data on π-d scattering at large backward angles were published by Schroeder et al.[23] for momenta above 496 MeV/c. Their data at 543 MeV/c can be compared directly with our data at 539 MeV/c, as the difference in momenta should result in only a 5% difference in cross sections. We show this comparison in Fig. 12. Our cross section at 156° is higher than theirs. Their data at 593 and 656 MeV/c were used to interpolate a backward angle point to compare to our data at 637 MeV/c, as shown in Fig. 13. Since we have no large measurement at this momentum, a direct comparison is not possible, but the combined data seem to indicate that the dip at around 100° observed at 441 and 539 MeV/c also appears at 637 MeV/c.

IV. COMPARISON WITH THEORETICAL CALCULATIONS

Next we compare our data to some theoretical calculations. Most of the calculations have been carried out specifically in the 3-3 resonance region, but some authors have presented results which can be compared to our data. Schiff and Tranh Thanh Van[4] published a relativistic calculation using a dispersion relation technique. Their calculations at 330 MeV (448 MeV/c) are compared with our data at 441 MeV/c in Fig. 11. The agreement seems satisfactory for the forward angles but the theoretical values are much too high for angles beyond 70° in the center of mass frame.

Very recent calculations by Ferreira et al.[1] have been carried out for both 343 and 441 MeV/c using a multiple scattering technique. Their results also tend to be higher than the experimental data especially at 343 MeV/c, as can be seen in Figs. 10 and 11. These authors believe the disagreement cannot be attributed to neglect of third- and higher-order scattering terms in the multiple expansion, because the second-order term does not make a strong contribution. Their calculations indicate that at large angles the cross sections are sensitive to deuteron structure (high momentum components in the wave function) and to detailed properties of the π-N and π-d interaction.

Rinat and Thomas[5] have carried out a relativistic calculation for the coupled $(\pi d, N\Delta)$ system, including specifically spin and isospin. Their calculation at 370 MeV/c is compared with our

data at 343 MeV/c in Fig. 10. Because of the momentum difference, one expects the theory to be approximately 20% lower than our data. Agreement is satisfactory at all angles.

Mandelzweig et al.[6] published a calculation based on the Faddeev equations, in which only the P_{33} πN channel was included, and the NN force in the intermediate states was neglected. The data of Gabathuler et al.[8] are fitted reasonably well in the forward direction but in the backward direction a calculated rising slope is too large to fit the experimental results. These authors believe that the backward behavior of their calculation can be attributed primarily to the use of only the P_{33} channel.

The π-d elastic scattering has also been studied in the Glauber approximation. Carlson[2] and Hoenig and Rinat[3] have published calculations in the energy region of our study. These calculations fit the data of Norem[7] quite well. They also fit the data of Gabathuler et al.[8] at lab angles less than ~80°. At large angles the data of Gabathuler are lower than the theory. Hoenig and Rinat also published curves for 438, 573, and 726 MeV/c. The first of these is compared with our 441 MeV/c data in Fig. 11. The second is compared with our 539 MeV/c data in Fig. 12. In this latter case, we expect that the difference in momenta for theory and experiment will result in the theory lying about 20% below the experimental points. Allowing for this, it can be seen that agreement with our data at the forward angles is good at both momenta, but the Glauber calculations tend to underestimate the backward cross section.

In conclusion, our data show a previously unobserved feature in the π-d elastic scattering cross section, namely a rather deep minimum around 100° which appears as the momentum increases above 340 MeV/c. Present calculations do not account for this dip. It would be tempting to say that it represents an interference between single and double scattering but the calculations of Ferreira et al.[1] do not support this hypothesis,

Improvement in the experimental accuracy and an increase in the number of data points along with a reduction in the momentum spread in the incident beam are the goals of our work presently under preparation. The continued improvement of the LAMPF intensity and operating characteristics since these data were taken make these realistic goals for the near future.

[1] E. M. Ferreira, L. Pinguelli Rosa, and Z. D. Thomé, Phys. Rev. C 16, 2353 (1977).
[2] C. Carlson, Phys. Rev. C 2, 1224 (1970).
[3] M. M. Hoenig and A. S. Rinat, Phys. Rev. C 10, 2102 (1974).
[4] D. Schiff and J. Tranh Thanh Van, Nucl. Phys. B3, 671 (1967).
[5] A. S. Rinat and A. W. Thomas, Nucl. Phys. A282, 365 (1977).
[6] V. B. Mandelzweig, H. Garcilazo, and J. M. Eisenberg, Nucl. Phys. A256, 461 (1976).
[7] J. H. Norem, Nucl. Phys. B33, 512 (1971).
[8] K. Gabathuler, C. R. Cox, J. J. Domingo, J. Rohlin, N. W. Tanner, and C. Wilkin, Nucl. Phys. B55, 397 (1973).
[9] G. B. Brunhart, G. S. Faughn, and V. P. Kenny, Nuovo Cimento 29, 1162 (1963).
[10] D. M. Lee, S. E. Sobottka, and H. A. Thiessen, Nucl. Instrum. Methods 109, 421 (1973).
[11] E. A. Wadlinger, Nucl. Instrum. Methods 134, 243 (1976).
[12] R. D. Werbeck and R. J. Macek (private communication).
[13] K. L. Brown, B. K. Kear, and S. K. Howry, Trans-port 1360, SLAC-91 (unpublished).
[14] R. Eisberg et al., Nucl. Instrum. Methods 21, 232 (1963).
[15] G. P. Millburn, W. Birnbaum, W. E. Crandall, and L. Schechter, Phys. Rev. 95, 1268 (1954).
[16] W. F. McGill et al., Phys. Rev. C 10, 2277 (1974).
[17] R. E. Pollock and G. Schrank, Phys. Rev. 140, B575 (1965).
[18] D. F. Measday and C. Richard-Serre, Nucl. Instrum. Methods 76, 45 (1969).
[19] F. Binon, P. Duteil, J. P. Garron, J. Gorres, L. Hugon, J. P. Peigneux, C. Schmit, M. Spighel, and J. P. Stroot, Nucl. Phys. 17B, 168 (1970).
[20] L. David Roper, R. M. Wright, and B. T. Feld, Phys. Rev. 138, B190 (1965).
[21] C. J. Bussey, J. R. Carter, D. R. Dance, D. V. Bugg, A. A. Carter, and A. M. Smith, Nucl. Phys. B68, 363 (1973).
[22] V. A. Gordeev et al., Yad. Fiz. 24, 1144 (1976) [Sov. J. Nucl. Phys. 24, 599 (1976)].
[23] L. S. Schroeder, D. S. Crabb, R. Keller, J. R. O'Fallon, T. J. Richards, R. J. Ott, J. Trischuk, and J. J. Vavra, Phys. Rev. Lett. 27, 1813 (1971).